

EFFECT OF INTENSIVE COOLING OF ALLOY AM60 WITH CHROMIUM AND VANADIUM ADDITIONS ON CAST MICROSTRUCTURE AND MECHANICAL PROPERTIES

The work presents the results of the investigations of the effect of intensive cooling of alloy AM60 with additions of chromium and vanadium on the microstructure and mechanical properties of the obtained casts. The experimental casts were made in ceramic moulds preliminarily heated to 180°C, into which alloy AM60 with the additions was poured. Within the implementation of the research, a comparison was made of the microstructure and mechanical properties of the casts obtained in ceramic moulds cooled at ambient temperature and the ones intensively cooled in a cooling liquid. The kinetics and dynamics the thermal effects recorded by the TDA method were compared. Metallographic tests were performed with the use of an optical microscope and the strength properties of the obtained casts were examined: UTS(Rm), elongation (A%), and HB hardness.

Keywords: investment casting, AM60, alloy additions, crystallization, intensive cooling

Introduction

Magnesium alloys, due to their relatively low mass, are more and more often applied in different branches of industry, especially the motor and aerospace industry [1]. These alloys characterize in a significantly lower mass than that of light aluminium alloys, but they also have much lower mechanical properties. In order to improve their mechanical properties, magnesium alloys are enriched with different alloy additions [2-8,12]. In the recent years, research has been made which confirms that a small amount of chromium and vanadium improves the properties of alloy AM60 [9]. To improve the mechanical properties of these alloys, new technologies are being developed, which characterize in directional crystallization assuring a rapid heat removal from the ceramic moulds [10,11]. The most popular ones, used to obtain titanium and aluminium casts, are two technologies: SOPHIA® [13] and HERO Premium Casting® [14]. The SOPHIA® technology has also been applied to obtain magnesium alloy casts [15].

The aim of this work was to examine the effect of intensive cooling of alloy AM60 with Cr and V additions on the microstructure, mechanical properties and HB hardness of experimental casts made in ceramic moulds intensively cooled in a cooling agent. The obtained test results for the casts which were intensively cooled in a cooling agent were compared with those of the casts cooled at ambient temperature.

Test methodology

The experiments were performed on alloy AM60 with the addition of 0.1% Cr and 0.1% V. The chemical composition of the initial alloy AM60 is given in Table 1.

TABLE 1

Chemical composition of alloy AM60

Chemical composition, % wt.							
Mg	Al	Zn	Mn	Si	Fe	Cu	Ni
93.697	6	0	0.23	0.05	0.004	0.008	0.001

According to the calculation, the alloy was enriched with master alloys AlCr15 and AlV10, whose chemical compositions are presented in Table 2 and 3.

TABLE 2

Chemical composition of master alloy AlCr15

Chemical composition, % wt.									
Mg	Al	Zn	Mn	Si	Fe	Cu	Ni	Cr	Other – max.
0.01	85.21	0.02	0.01	0.08	0.25	0.01	0.01	14.2	0.2

TABLE 3

Chemical composition of master alloy AlV10

Chemical composition, % wt.				
Al	V	Si	Fe	Other – max.
89.654	9.69	0.215	0.241	0.2

* LODZ UNIVERSITY OF TECHNOLOGY, DEPARTMENT OF MATERIALS ENGINEERING AND PRODUCTION SYSTEMS, 1/15 STEFANOWSKIEGO STR., 90-924 ŁÓDŹ, POLAND.

[#] Corresponding author: cezary.rapiejko@p.lodz.pl

The alloy was melted in a laboratory crucible resistance furnace, capacity 5 kg, in a crucible made of steel S235JRG2 (PN-EN 10025-2:2007). Inside the furnace, a protective gas atmosphere was used, consisting of a mixture of Ar + SF₆, pressure 0.15-0.20 MPa. The gas flow equaled: 10 cm³/min for SF₆ and 500 cm³/min for Ar. Due to the high tendency of the chromium and vanadium additions for gravitational segregation, the magnesium alloy with the additions was intensively mixed in the crucible.

The cylindrical casts of the samples for strength tests were made in ceramic moulds produced according to the lost mould casting method. The prepared ceramic mould is shown in Figure 1.



Fig. 1. Ceramic mould for strength tests casts

The moulds were made of Refracoarse refractory materials (flour and sands). The latter consisted of 7 coatings applied in mixers and a fluidizer in the foundry „Armatura” Lodz, Poland. Each coating was created as a result of applying a binder on a wax model, and next covering the latter with quartz sand of a specific granularity. The configuration and type of the applied coatings were discussed in work [16]. After the ceramic mould had been dried, the model mass was melted out of it in an autoclave at 150°C. Next, the mould was burnt at 960°C in a tunnel furnace. After the burning process, the ceramic moulds were cooled down to 180°C, and then the liquid metal of 740°C ±5°C was poured in. The moulds filled with the liquid alloy, after the solidification of about 30% of the alloy volume in a random micro-volume of the casts, were submerged in a cooling agent at the rate of $V = 0.08$ m/s. As the cooling agent a 20%

solution of Polihartenol E8 in water was used, at the ambient temperature $t_{at} = 20^\circ\text{C}$. The solidification time of 30% of the alloy volume in a random cast volume was determined with the use of the Magma5 software. In the program, the properties of the magnesium alloys were defined based on the data from the Magma5 system data base:

- alloy AM60B,
- time of pouring the mould with the metal: 4 s,
- temperature of the liquid metal during pouring: 740°C,
- mould made of aluminium oxide: Al₂O₃,
- temperature of the ceramic mould: 180°C.

After pouring, the moulds cooling at ambient temperature were placed on a cooling station.

The examinations of the process of solidification and crystallization of alloy AM60 with the alloy additions were performed in specially designed and produced ceramic samplers TDA10C-PL with the use of the TDA method. The construction of the samplers and the schematics of the TDA method testing station for the alloys cooling at ambient temperature have been described in work [17]. The schematics of the TDA method testing station of the alloys intensively cooled in a cooling agent have been discussed in work [18].

Evaluation of the following crystallization processes was performed by the TDA method: cooling ($t = f(\tau)$), kinetics ($dt/d\tau = f'(\tau)$) and dynamics ($d^2t/d\tau^2 = f''(\tau)$). On the derivative curve $dt/d\tau = f'(\tau)$, characteristic points were determined, which were then used to determine the thermal effects of crystallization for the selected alloy:

- A-D – crystallization of primary phase α_{Mg} ($L \rightarrow L + \alpha_{\text{Mg}}$),
- D-E-F-I – crystallization of eutectics $\alpha_{\text{Mg}} + \gamma$ ($\text{Mg}_{17}\text{Al}_{12}$) ($L \rightarrow \alpha_{\text{Mg}} + \gamma$ ($\text{Mg}_{17}\text{Al}_{12}$)).

For the description of the characteristic thermal effects occurring during primary crystallization, the quantities determined for the characteristic points were used:

- alloy temperature t , °C,
- value of the first derivative of temperature after time $dt/d\tau$, °C/s,
- time τ from the beginning of the measurement to the recording of a characteristic point on the derivation curve ($dt/d\tau$), s,
- value of the tangent of the inclination angle of the straight line on the interpolator interval between the characteristic points $Z = \text{tg}(\alpha) \approx d^2t/d\tau^2$, °C/s².

In order to show the particular phases in the microstructure, the microsections were etched with a reagent of the following composition: 1 ml acetic acid, 50 ml distilled water and 150 ml ethyl alcohol [19]. The microstructure of the examined alloys was observed with the optical microscope Nikon Eclipse MA200.

The examinations of the selected mechanical properties, i.e.: R_m , $A_{\%}$, were performed for samples of cylindrical casts, according to the standard EN-ISO 6892/1, by means of the testing machine Instron 4485. Hardness measurements were conducted by the Brinell method, determining the HB hardness, with the loading force $F = 490$ N, the penetrator (nodule) diameter $d = 2.5$ mm and the load factor $k = 10$.

1. Discussion of results

1.1. Microstructure of alloy AM60 with Cr and V additions cooling at ambient temperature and intensively cooled

Figure 2a,b shows the microstructure of alloy AM60 with chromium and vanadium additions cooling in a ceramic mould at ambient temperature. The alloy microstructure consists of the following phases: α_{Mg} + eutectic ($\alpha_{Mg} + \gamma(Mg_{17}Al_{12})$), AlMn. The introduced additions of Cr and V dissolved in the matrix and, above all, in the intermetallic phase $Mg_{17}Al_{12}$.

A very strong effect on obtaining an alloy microstructure without porosity defects, caused by the ceramic mould being penetrated by the water vapour, is exhibited by the participa-

tion of the solid phase in the cast at the moment of initiation of intensive cooling of the mould. The performed simulations of the process of ceramic mould pouring and alloy solidification, with the use of the MAGMA5 software, as well as the validation of the simulation results under laboratorial conditions made it possible to determine the time that should pass from the moment of mould pouring to the moment of submerging the mould in the cooling agent. This time is necessary for the formation of a solidified phase in the volume of the mould shaping the cast which is strong enough to withstand the pressure of the gases trying to get to the liquid alloy. Based on these tests, it was assumed that the formation of a 30% solid phase in the alloy, in the area of the mould shaping the cast, makes it possible to obtain cylindrical casts without defects caused by porosity. Figures 3a,b

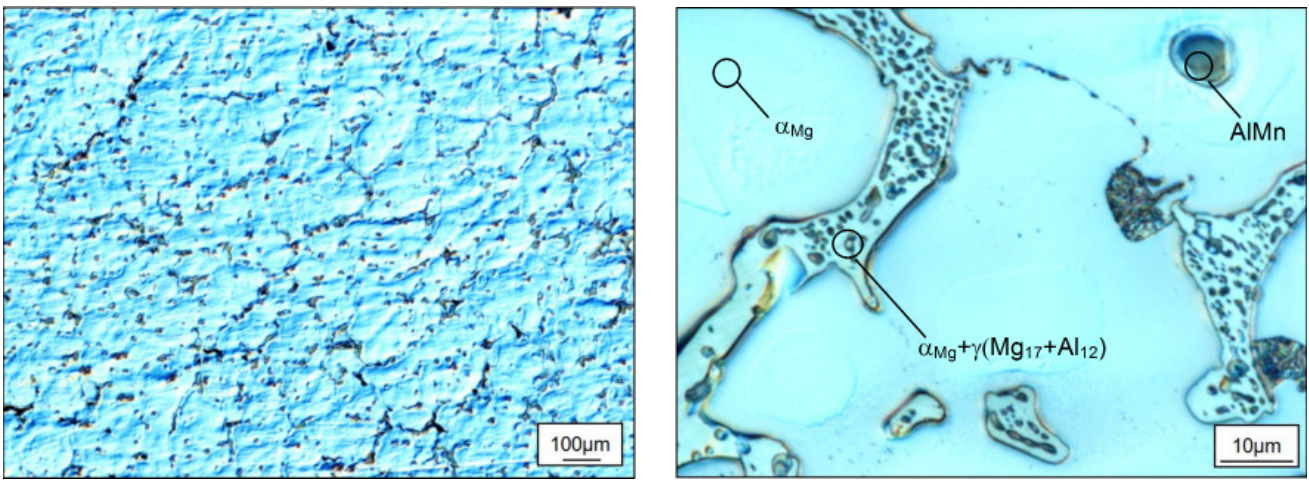


Fig. 2. Microstructure of alloy AM60 with chromium and vanadium additions solidifying in an TDA sampler at ambient temperature

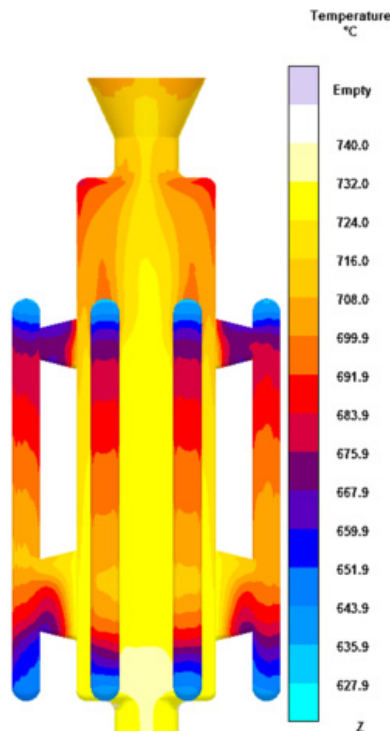


Fig. 3a. Cast temperature at the moment of mould pouring with alloy AM60B

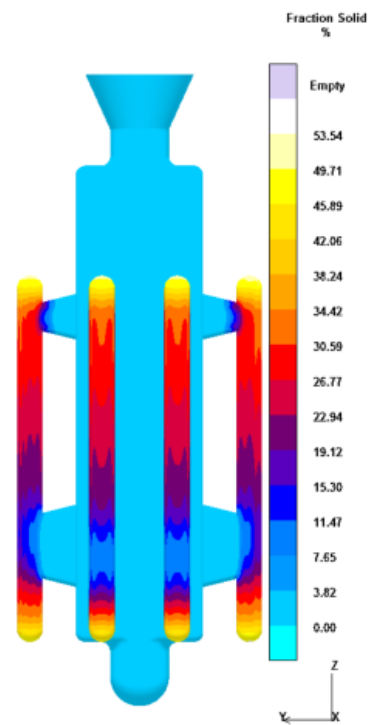


Fig. 3b. Amount of solid phase in the case of alloy AM60B, after solidification time $t = 15,179$ s

present the simulation results of: the temperature distribution of alloy AM60B after pouring the mould of cylindrical casts (a), the percentage of the solid phase in the volume of the cast made of alloy AM60B (b). From the presented simulation of the temperature distribution of the cylindrical cast right after mould pouring (Fig. 3a) it can be inferred that the coolest areas of the cast are its edges. In these areas, the temperature of the liquid alloy is in the range of 651.9-643.9°C. In the volume of

the cylindrical cast, after ca. 15.2 s from the moment of mould pouring (3b), large areas were observed with about 30% of solid phase in the cast volume.

Figure 4 shows the microstructure of alloy AM60 with chromium and vanadium additions, intensively cooled in a ceramic mould at ambient temperature. The alloy microstructure consists of the following phases: α_{Mg} + eutectic ($\alpha_{Mg} + \gamma(Mg_{17}Al_{12})$) saturated with alloy additions (Cr and V).

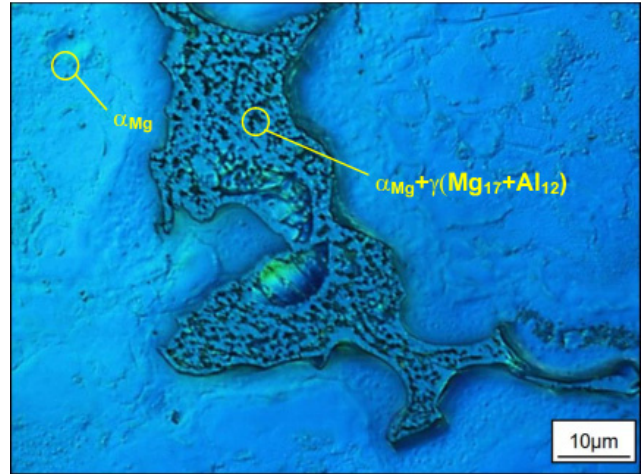
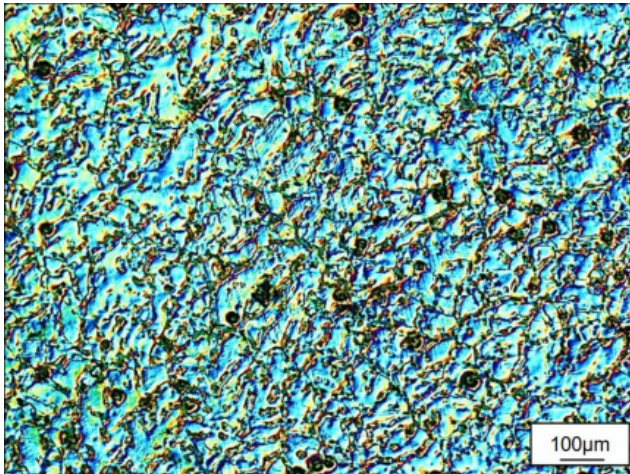


Fig. 4. Microstructure of alloy AM60 with chromium and vanadium additions solidifying in an intensively cooled ceramic TDA sampler

1.2. TDA analysis

Figure 5 shows the characteristics of alloy AM60 with additions of chromium and vanadium, solidifying in an TDA sampler at ambient temperature and intensively cooled in a water solution of Polihartenol E8.

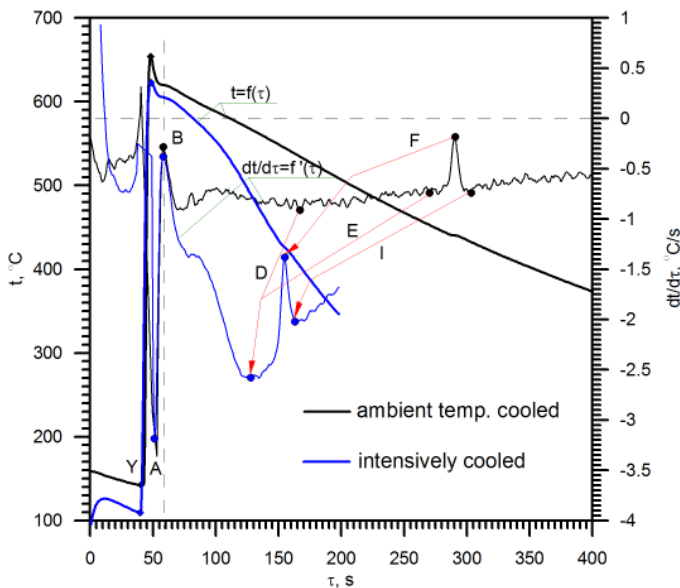


Fig. 5. TDA characteristics of alloy AM60 with chromium and vanadium additions solidifying in a ceramic TDA sampler at ambient temperature and intensively cooled

Tables 4 and 5 present compilations of $(t, dt/d\tau, d^2t/d\tau^2)$ determined for characteristic points or segments formed by these points ($Z \approx d^2t/d\tau^2$) from the TDA curves for the examined alloys.

On the derivation curve $(dt/d\tau)$, points A, D and E determine the thermal effect of the crystallization of phase α_{Mg} in the volume of the sampler; E-I determine the thermal effect of the crystallization of eutectic $\alpha_{Mg} + \gamma(Mg_{17}Al_{12})$. After the metal has been supercooled below the equilibrium liquidus temperature t_A . The thermal effect A-B-D includes the stage of intensive nucleation and growth of phase α_{Mg} , whose intensity drops on the segment between points D and E. At this stage, before the crystallization front of phase α_{Mg} , the concentration of Al slowly increases in the liquid alloy, which, in consequence, leads to nucleation and growth of eutectic $\alpha_{Mg} + \gamma(Mg_{17}Al_{12})$. After the metal has been supercooled below the equilibrium temperature of eutectic transformation, at the actual transformation temperature t_F , eutectic $\alpha_{Mg} + \gamma(Mg_{17}Al_{12})$ nucleates and grows. Alloy AM60 with the additions solidifies in the volume of the TDA10C-PL sampler at point I. Intensive cooling of alloy AM60 with the additions caused changes in the kinetics and dynamics of the thermal processes, as compared to the alloy solidifying at ambient temperature, which, in consequence, shortened the time of nucleation of phase α_{Mg} and growth of eutectic $\alpha_{Mg} + \gamma(Mg_{17}Al_{12})$. The difference in the solidification time of the alloy within the volume of the sampler between the alloy cooled at ambient temperature and the one intensively

TABLE 4

Characteristic TDA points and their corresponding values: $t = f(\tau)$, $dt/d\tau = f'(\tau)$, $d^2t/d\tau^2 = f''(\tau)$, $Z \approx (d^2t/d\tau^2) \cdot 10^{-3}$ for alloy AM60 with chromium and vanadium additions solidifying in TDA10C-PL sampler at ambient temperature

Point	τ , s	t , °C	$dt/d\tau$, °C/s	$d^2t/d\tau^2$, °C/s ²	$Z \approx d^2t/d\tau^2 \cdot 10^{-3}$, °C/s ²
A	50.6	638.4	-6.062	0.2667	585.99
B	58.2	619.8	-0.284	0.0056	212.77
D	167.0	534.5	-0.913	0.0137	-23.25
E	270.1	452.9	-0.739	-0.0261	5.17
F	290.6	440.3	-0.185	-0.0573	99.41
I	303.4	432.4	-0.741	0.0329	5.40

TABLE 5

Characteristic TDA points and their corresponding values: $t = f(\tau)$, $dt/d\tau = f'(\tau)$, $d^2t/d\tau^2 = f''(\tau)$, $Z \approx (d^2t/d\tau^2) \cdot 10^{-3}$ from alloy AM60 with chromium and vanadium additions solidifying in TDA10C-PL sampler, intensively cooled

Point	τ , s	t , °C	$dt/d\tau$, °C/s	$d^2t/d\tau^2$, °C/s ²	$Z \approx d^2t/d\tau^2 \cdot 10^{-3}$, °C/s ²
A	53.1	615.9	-3.186	-0.1150	569.25
B	60.1	605.2	-0.380	0.0016	137.20
D	129.9	489.5	-2.577	-0.0009	-6.18
E	129.9	489.5	-2.577	-0.0009	-6.18
F	156.8	426.5	-1.382	-0.0225	185.37
I	165.1	411.7	-2.020	-0.0052	5.07

cooled equals $\Delta\tau_{A-I} = \tau_{A-I \text{ ambient}} - \tau_{A-I \text{ intensively}} = (303.4 - 50.6) - (161.1 - 53.1) = 144.8$ s, where the crystallization time of phase α_{Mg} shortened $\Delta\tau_{A-E} = \tau_{A-E \text{ ambient}} - \tau_{A-E \text{ intensively}} = (270.1 - 50.6) - (129.9 - 53.1) = 142.7$ s, and the crystallization time of the growth of eutectic $\alpha_{Mg} + \gamma(Mg_{17}Al_{12})$ shortened $\Delta\tau_{E-I} = \tau_{E-I \text{ ambient}} - \tau_{E-I \text{ intensively}} = (303.4 - 270.1) - (165.1 - 129.9) = 1.9$ s.

1.3. Strength properties R_m , A_5 and HB hardness

Figure 6 shows a diagram of the tensile strength R_m of alloys AM60 with chromium and vanadium additions, cooled at ambient temperature and intensively cooled in a water solution of Polihartenol.

From the diagram presented in Figure 6 it can be inferred that the intensive cooling caused an increase of the tensile strength by 5 MPa, which constitutes an increase of the tensile strength of the cast by about 4%. Figure 7 shows a diagram of elongation A_5 of alloys AM60 with chromium and vanadium additions cooled at ambient temperature and intensively cooled in a water solution of Polihartenol.

From the diagram presented in Figure 7 it can be inferred that the intensive cooling caused a reduction of elongation A_5 by 0.2%, which constitutes a drop of elongation of the cast by about 12%.

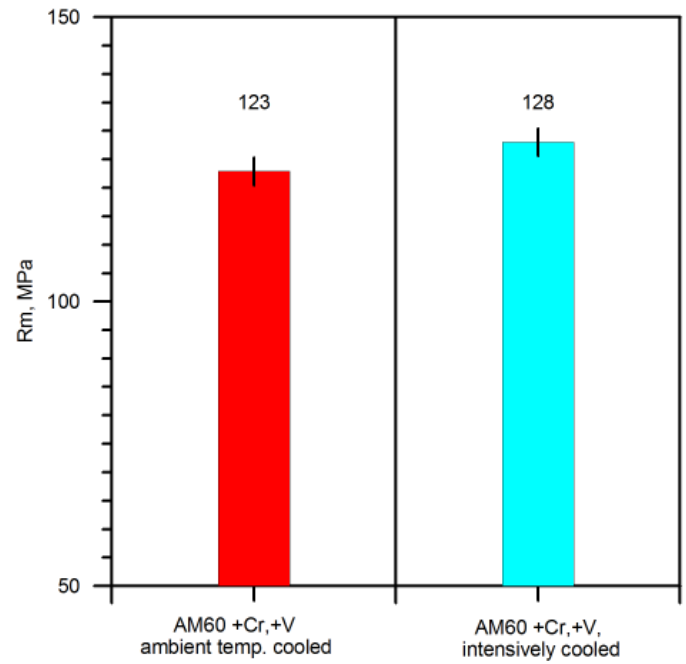


Fig. 6. Tensile strength R_m of alloy AM60 with chromium and vanadium additions solidifying in a ceramic mould at ambient temperature and intensively cooled

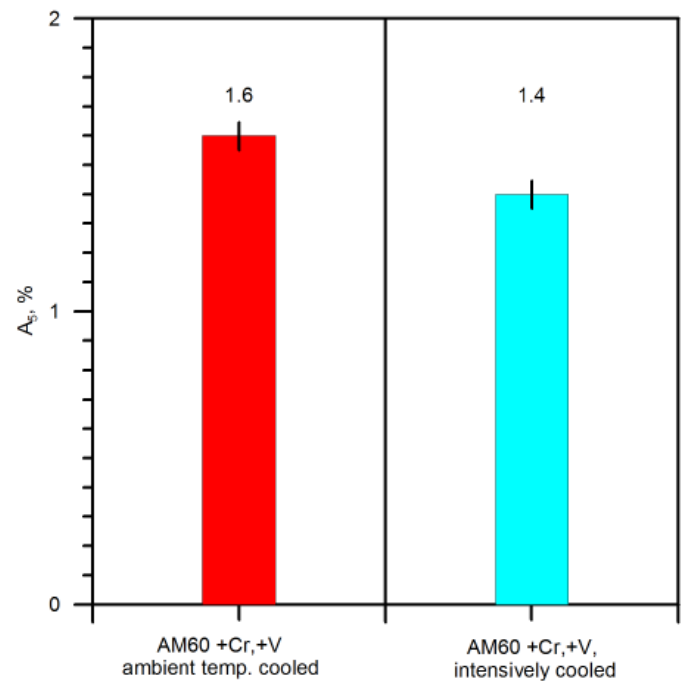


Fig. 7. Elongation A_5 of alloy AM60 with chromium and vanadium additions solidifying at ambient temperature and intensively cooled

Figure 8 shows the distribution of hardness HB of alloys AM60 with chromium and vanadium additions cooled at ambient temperature and intensively cooled in a water solution of Polihartenol.

From the diagram presented in Figure 8 of the distribution of hardness HB it can be inferred that the intensive cooling caused an increase of hardness HB by about 3%.

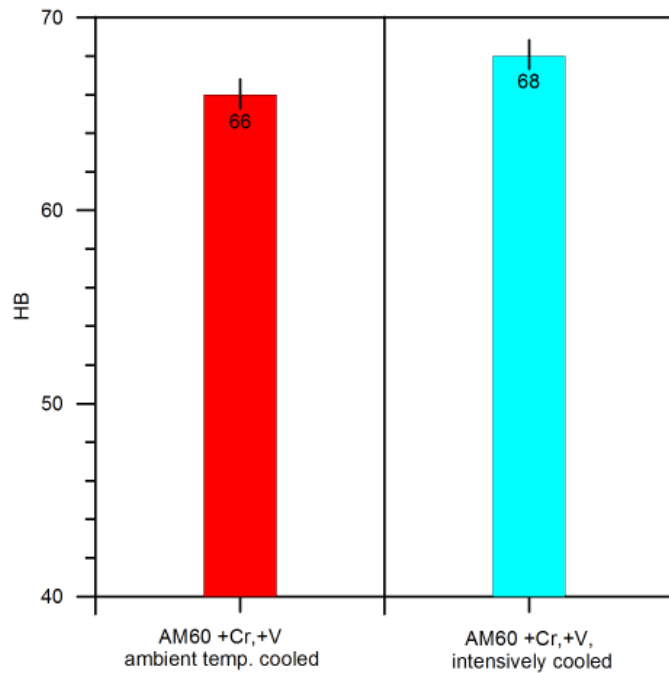


Fig. 8. HB hardness of alloy AM60 with chromium and vanadium additions solidifying at ambient temperature and intensively cooled

2. Conclusions

Based on the performed research, we can conclude that the application of intensive cooling of alloy AM60 with chromium and vanadium additions caused:

- shortening of the primary crystallization time of the alloys with a magnesium matrix by about 50%,
- refinement of phase α_{Mg} , refinement of massive precipitations $\gamma(Mg_{17}Al_{12})$ and refinement of eutectic $\alpha + \gamma(Mg_{17}Al_{12})$,
- increase of the strength properties R_m by about 4%,
- reduction of the relative elongation A_5 by about 12%,
- increase of the HB hardness by about 3%.

Acknowledgements

This work was realized within the frames of Project PBS I, financed by the National Centre for Research and Development, Poland. Project ID: 178739. Project implemented in 2013-2015.

REFERENCES

- [1] K.U. Kainer, Magnesium: Proceedings of the 7th International Conference on Magnesium Alloys and Their Applications. 2007 Wiley-VCH, Weinheim.
- [2] A. Boby, K.K. Ravikumar, U.T.S. Pillai, B.C. Pai, Proc. Eng. **55**, 98-102 (2013).
- [3] Y. Chen, H. Liu, R. Ye, G. Liu, Mater. Sci. Eng. A **587**, 262-267 (2013).
- [4] H. Sevik, S. Acıkgöz, S.N. Kurnza, J. Alloy Compd. **508**, 110-114 (2010).
- [5] S. Candan, M. Unal, E. Koc, Y. Turen, E. Candan, J. Alloys Comp. **509**, 1958-1963 (2011).
- [6] N. Balasubramani, A. Srinivasan, U.T.S. Pillai, K. Raghukandan, B.C. Pai, J. Alloys Compd. **455**, 168-172 (2007).
- [7] A. Srinivasan, U.T.S. Pillai, B.C. Pai, Metall. Mater. Trans. A **36A**, 2235-2243 (2005).
- [8] K.Y. Nam, D.H. Song, C.W. Lee, Mater. Sci. Forum **510-511**, 238-241 (2006).
- [9] C. Rapijko, B. Pisarek, T. Pacyniak, Arch. Metall. Mater. **59** (2), 761-765 (2014).
- [10] R. Władysiak, Arch. Metall. Mater. **52** (3), 529-534 (2007).
- [11] R. Władysiak, A. Kozuń, T. Pacyniak, Arch. Found. Eng. **16** (1), 89-94 (2016).
- [12] K. Neh, M. Ullmann, R. Kawalla, Mater. Today Proc. **2**, 219-224 (2015).
- [13] J. Gabriel, ZGV-ZENTRALE FUER GUSSVERWENDUNG **21** (1), 4-10 (1996).
- [14] Ch. Liesner, R. Gerke-Cantow, ZGV-ZENTRALE FUER GUSSVERWENDUNG **27** (2), 41-44 (2002).
- [15] <http://www.aeromet.co.uk/casting-division/index.html>
- [16] S. Pietrowski, C. Rapijko, Arch. Found. Eng. **11** (3), 177-186 (2011).
- [17] C. Rapijko, B. Pisarek, E. Czekaj, T. Pacyniak, Arch. Metall. Mater. **59** (4), 1449-1455 (2014).
- [18] C. Rapijko, B. Pisarek, T. Pacyniak, Arch. Found. Eng. **14** (1), 97-102 (2014).
- [19] A. Maltais, D. Dube, M. Fiset, G. Laroche, S. Tugeon, Mater. Char. **52**, 103-119 (2004).